

Design of Passive-Type Radar Reflector

Jeong-Bin Yim* · Woo-Suk Kim*

* ,** Division of Maritime Transportation System, Mokpo National Maritime University, Mokpo, 530-729, Korea

Abstract : This paper describes design method of Passive-type Radar Reflector (PRR) which is to provide the requirement of newly revised 2000 SOLAS regulations on the Radar Reflector. The main target of this work is to find the optimum shape of a radar target having large Radar Cross Section (RCS). Through the RCS analysis based on the theoretical approach, two kinds of PRR models, PRR-F model for use in fisheries and PRR-S model for use in small sized ship, are designed and discussed their RCS performance. RCS measurement tests for the various sized samples are carried out in an anechoic chamber. As evaluation results it was clearly shown that the conventional sphere-type shows optimum shape in case of PRR-S, while the cylinder-type which consists of large sized corner clusters or zig-zag flat plats gives best performance in case of PRR-F.

Key words : passive-type radar reflector, optimum target shape, SOLAS 2000, Radar Cross Section, reflector modeling

1. Introduction

On 14 April 1912, Titanic foundered and safety standards in the shipbuilding changed forever. Soon after the tragedy, the International Maritime Organization (IMO) was established to investigate maritime laws and regulations. The IMO prompted the first Safety Of Life At Sea (SOLAS) conference. SOLAS represented an international agreement to secure the protection of life at sea. Then, the SOLAS chapter V was revised with several relevant resolutions in July 2000. These amendments entered into force on 1 July 2002. Consequently, the craft of 150 tonnage or below shall be provided with a radar reflector, or other means, to assist detection by ships navigating by radar at both 9 and 3 GHz (IMO, 1973; IMO, 1977; IMO, 2000).

Most of the small and medium sized vessel, with wood and fiberglass hulls, even those with metal masts and engines, do not possess enough reflective qualities to make them highly visible on a radar screen. In addition, small radar reflectors may not show up on a ship as radar, due to rain or background wave clutter. The fishing buoy, with styrofoam and nylon material, has also same problems as the small sized vessel.

The conventional Passive-type Radar Reflector (PRR) is made of three planar circles or squares of metal intersecting at right angles, forming eight trihedral reflectors, known as octahederal. An essential design feature of a reflector, which greatly enhances the effective amount of signal returned, is the accuracy of the right angles formed between the plates.

The other thing that is key to the performance of any reflector design is size. The reflective performance of any

type of reflector is proportional to the fourth power of its linear size. In other words, doubling the size of a reflector results in an increase of effective area of 16 times, or a 12 dB increase. Further, as the smallest dimension of a reflector gets down to a few wavelengths of the radar signal, it quits acting as a reflector and starts to act as a lump of metal. So small detectors must be looked at with a great deal of suspicion, as there really is no substitute for size.

In addition, the reflector shape is also important factor that could give an optimum performance of a reflector. Sphere-type is a usual shape in the conventional PRR. While, in the view point of RCS (Radar Cross Section) performance, the other types, such as cylinder-type, zig-zag-type, *etc.*, may give more high quality RCS than that of the conventional ones (J. B. Yim, 2002a; J. B. Yim, 2002b).

With those considerations, several radar targets are analysed based on the theoretical RCS approach, and the two kinds of PRR models are designed for the use of fisheries (PRR-F) and for the use of small sized ship (PRR-S). Further, RCS measurement tests for the various sized samples are carried out in an anechoic chamber. In the evaluation process, In this test, Model-153 Davis Echomaster is used as a reference reflector. The Model-153 is known as the best PRR in a commercial market.

2. RADAR TARGET DESIGN

2.1 Radar Cross Section

When radar signals are reflected from irregular surfaces,

* Corresponding Author : Jeong-Bin Yim, jbyim@mmu.ac.kr 061)240-7051

** wskim@mmu.ac.kr 061)240-7059

such as buoys, sailboats and runabouts, they will rebound in many directions, leaving only a small portion to be reflected in the direction of the radar observer. Obviously, some standard had to be used in making meaningful comparisons of various reflective surfaces. The term 'effective radar cross-section', referred to as RCS (Radar Cross Section), has been adopted worldwide in making comparisons of reflective surfaces as shown in Fig. 1 (E. F. Knott, 1993; J. Coreman *etc*, 1995).

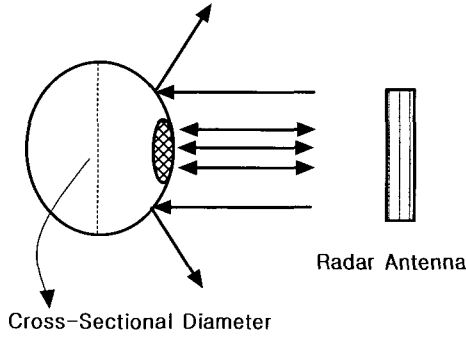


Fig. 1 A metal sphere to indicate RCS

In general, marine radar classified into two bands, X-band and S-band. Large vessels will typically carry both, while small vessels are limited to the smaller X-band radar. X-band radar operates at a frequency of approximately 9.4 GHz, with a wavelength of 3.2 cm, while S-band operates at approximately 3.0 GHz, with a longer wavelength of 10.0 cm. X-band radar offers greater resolution and detection of smaller targets, but is more susceptible to interference from rain and seas. S-band radar has longer range and less interference from rain and sea clutter, but has less sensitivity for small targets. Thus, the size of reflector will be more large one to get a good performance at both X and S bands.

2.2 RCS Theory

Assume the power density of a wave incident on a target located at range R away from the radar is P_{Di} . The amount of reflected power from the target is (W. S. Kim *etc*, 2002)

$$P_r = \sigma P_{Di} \quad (1)$$

σ denotes the target cross section (RCS). Define P_{Dr} as the power density of the scattered waves at the receiving antenna. It follows that

$$P_{Dr} = \frac{P_r}{4\pi R^2} \quad (2)$$

Equating Eqs. (1) and (2) yields

$$\sigma = 4\pi R^2 \left(\frac{P_{Dr}}{P_{Di}} \right) \quad (3)$$

and in order to ensure that the radar receiving antenna is in the far field, *i.e.*, scattered waves received by the antenna are planar, Eq. (3) is modified

$$\sigma = 4\pi R^2 \lim_{R \rightarrow \infty} \left(\frac{P_{Dr}}{P_{Di}} \right) \quad (4)$$

The RCS defined by Eq. (4) is often referred to as either the monostatic RCS, the backscattered RCS, or simply target RCS (A. K. Bhattacharyya and D. L. Sengupta, 1991; M. L. Skolnik, 2001). The backscattered RCS is measured from all waves scattered in the direction of the radar and has the same polarization as the receiving antenna. It represents a portion of the total scattered target RCS σ_t , where $\sigma_t > \sigma$. Assuming spherical coordinate system defined by (ρ, θ, ϕ) then at range ρ the target scattered cross section is a function of (θ, ϕ) . Let the angles (θ_i, ϕ_i) define the direction of propagation of the incident waves. Also, let the angles (θ_s, ϕ_s) define the direction of propagation of the scattered waves. The special case, when $\theta_s = \theta_i$ and $\phi_s = \phi_i$ defines the monostatic RCS. The RCS measured by the radar at angles $\theta_s \neq \theta_i$ and $\phi_s \neq \phi_i$ is called the bistatic RCS. The total target scattered RCS is given by

$$\sigma_t = \frac{1}{4\pi} \int_{\phi_s=0}^{2\pi} \int_{\theta_s=0}^{\pi} \sigma(\theta_s, \phi_s) \sin \theta_s d\theta d\phi_s \quad (5)$$

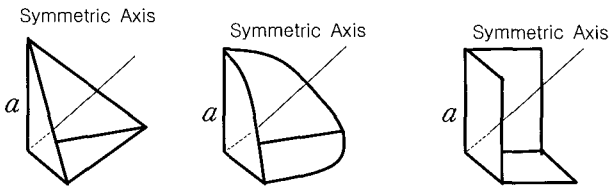
The amount of backscattered waves from a target is proportional to the ratio of the target size to the wavelength, λ , of the incident waves. In fact, a radar will not be able to detect targets much smaller than its operating wavelength.

The analysis presented in this work assumes far field monostatic RCS measurements in the optical region. Thus, near field RCS, bistatic RCS, and RCS measurements in the Rayleigh region are not be considered. Additionally, RCS treatment in this work is mainly concerned with narrow band cases.

2.3 Analysis of Radar Targets

Fig. 2 shows three kinds of tri-hedral complex radar targets. A complex target RCS is normally computed by coherently combining the cross sections of the simple shapes that make that targets. In general, a complex target RCS can be modeled as a group of individual scattering centers distributed over the target. Due to the difficulties

associated with the exact RCS prediction for the complex radar target, approximate methods become the viable alternative (B. R. Mahafza, 2000).



(a) Triangular-type (b) Circular-type (c) Rectangular-type

Fig. 2 Complex radar targets

The following equations are approximated maximum RCS (σ_{max}) at given conditions. Eqs. (6), (7), and (8) correspond to complex targets as shown in Fig. 2(a), (b), and (c), respectively (SMI, 2001; NIST, 2002; Ohio Univ., 2002a; Ohio Univ., 2002b).

$$\sigma_{max} = \frac{4\pi a^2}{3\lambda^2} = 4.19 \frac{a^2}{\lambda^2} \quad (6)$$

$$\sigma_{max} = \frac{16\pi a^2}{3\lambda^2} = 15.61 \frac{a^2}{\lambda^2} \quad (7)$$

$$\sigma_{max} = \frac{12\pi a^2}{\lambda^2} = 37.67 \frac{a^2}{\lambda^2} \quad (8)$$

and maximum radar range R_{max} is given by

$$R_{max} = \left[\frac{P_t G^2 \lambda^2 \sigma}{(4\pi)^3 S_{min}} \right]^{1/4}, \quad (9)$$

where P_t : peak transmitted power, G : antenna gain, λ : wave length, σ : RCS, S_{min} : minimum detectable signal power.

Related maximum RCS σ_{Rmax} and related maximum radar detection range R_{Rmax} , calculated from Eqs. (6), (7), (8), and (9) are summarized as in Table 1.

Table 1 Calculated σ_{Rmax} and R_{Rmax}

Configuration	Related maximum RCS, σ_{Rmax}	Related maximum radar detection range, R_{Rmax}
Triangular tri-hederal	1.0	1.0
Circular tri-hederal	3.7	1.4
Rectangular tri-hederal	8.9	1.7

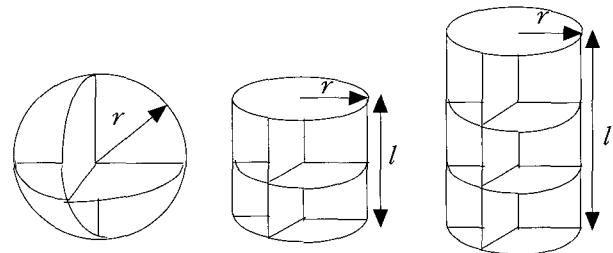
In Table 1, the order of large σ_{Rmax} is rectangular tri hederal, circular tri-hederal and triangular tri-hederal.

Moreover, it is seen that σ_{Rmax} increases very rapidly as radar reflector dimensions are increased since σ_{Rmax} varies as the 4th power of dimension. However, in case of radar detection range R_{Rmax} , increases much more slowly since R_{Rmax} varies inverse 4th power of σ . Thus, doubling the size of the radar reflector will not usually double the detection range.

2.4 Design of Radar Reflectors

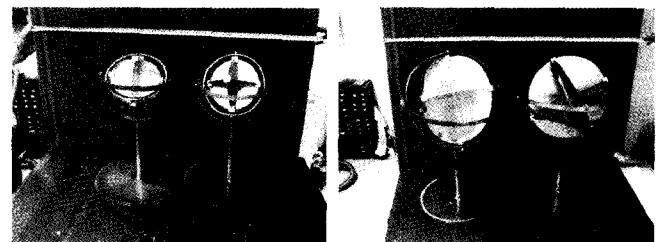
The important fact in reflector design is that the rectangular flat plate is seldom used in marine systems due to its non-compatibility with sails and rigging, and also due to its extra weight and high vulnerability to windage. However there is no substitute for size when it comes to radar reflectors.

To find optimum radar targets, several design samples of PRR-S and PRR-F are tested and analysed for their RCS performance. Fig. 3 shows the geometry associated with a sphere and a cylinder as basic design models, and their test samples are representing in Fig. 4 and Fig. 5.



(a) Sphere-type (b) Cylinder-type (c) Double cylinder-type

Fig. 3 Basic design geometry of PRR-S and PRR-F



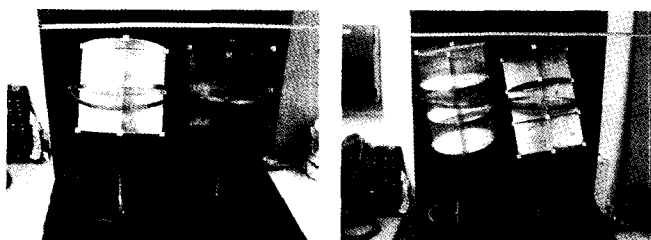
(a) Sphere, $r=7.5\text{cm}$

(b) Sphere, $r=15\text{cm}$



(c) Cylinder, $r=7.5\text{cm}$, $l=15\text{cm}$,

(d) Double Cylinder, $r=7.5\text{cm}$, $l=22.5\text{cm}$



(e) Cylinder, $r=15\text{cm}$, $l=30\text{cm}$ (f) Double Cylinder, $r=15\text{cm}$, $l=45\text{cm}$

Fig. 4 Test samples of PRR-S

The plate material of PRR-S is aluminum or bronze, and that of the PRR-F is galvanized iron sheet to provide high buoyance fishing buoy by take off weight. Three or more planar circles or squares intersecting at right angles are used in the construction of PRR-S. In case of PRR-F's in Fig. 5(a) and (b) arrayed corner clusters which are attached to the surface of styrofoam fishing buoy are used. While in case of the PRR-F's in Fig. 5(c) and (d) arrayed corner clusters are surrounded with styrofoam.



(a) 4-stage cylinder with small sized corner cluster, $r=19\text{ cm}$, $l=43\text{ cm}$

(b) 3-stage cylinder with medium sized corner cluster, $r=26\text{ cm}$, $l=93\text{ cm}$



(c) 3-stage cylinder with medium sized zig-zag block, $r=26\text{ cm}$, $l=93\text{ cm}$

(d) 3-stage cylinder with large sized zig-zag block, $r=39\text{ cm}$, $l=140\text{ cm}$

Fig. 5 Test samples of PRR-F

3. Experiments and Evaluations

3.1 Experimental Environment

The tests were conducted in an anechoic chamber of Korea Maritime University, Korea. The target is centered near the far end of the chamber, on a radar-transparent

plate that can be rotated through 360° manually. A calibrated broadband microwave transmitter/receiver is located in the wall at the opposite end of the chamber to accurately measure the reflected signal as shown in Fig. 6.

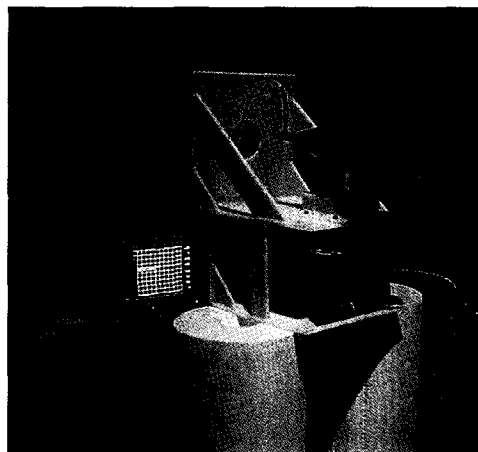


Fig. 6 Test environment

The walls, ceiling and floor are covered with semi-conductive, radar absorbing foam pyramids which absorb any stray radar signals and prevent any reflections back to the receiver, except those from the device under test.

The chamber is optimized to measure the very small radar returns. The background return is on the order of -60 dB . Calibration was checked before each days testing.

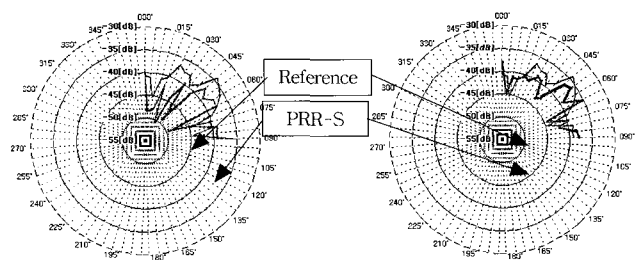
A microcomputer provided data logging. Data was taken simultaneously at 9.4 GHz , recorded directly to disc and plotted to a printer. The data was subsequently converted to text files and transferred to floppy disc files for further analysis.

3.2 Test Results

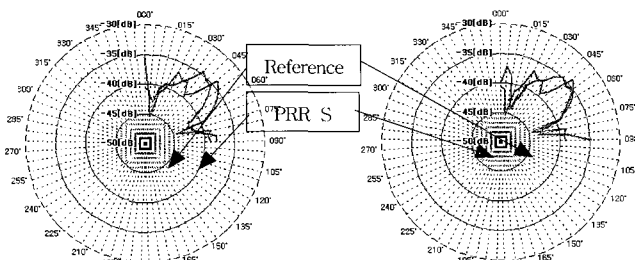
The test results of selected individual samples of PRR-S and PRR-F are shown in graphical form as Fig. 7 and Fig. 8, respectively. The obtained gain in dB is shown as polar plots for X-band only, indicating the strength of the reflected signal in that would be seen by a ship. Due to roll symmetry of PRR-S and PRR-F, test results show only a quarter of 360° in Fig. 7, and a half of 360° in Fig. 8. In the both of Fig. 7 and Fig. 8, measured gain of test sample is compared with the Davis Echomaster Model-153, known as RCS 12m^2 , radius $r=15\text{ cm}$, weight 0.79 kg , plate material 1.27 mm marine grade aluminum plates (Davis, 2002).

With regard to the test samples of PRR-S in Fig. 7(a) and (b), the models tested show poor performance compared with a reference model (Davis Echomaster). While, Fig. 7(c) and (d) give more or less performance than that of the

reference model. It is to be considered that the PRR-S's in Fig. 7(c) and (d) has larger size than the reference model.

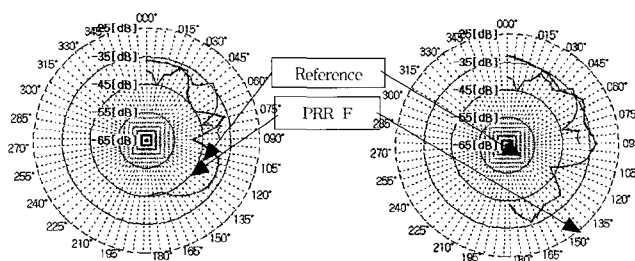


(a) Sphere, Bronze, $r=7.5$ cm (b) Cylinder, Bronze, $r=15$ cm, $l=30$ cm



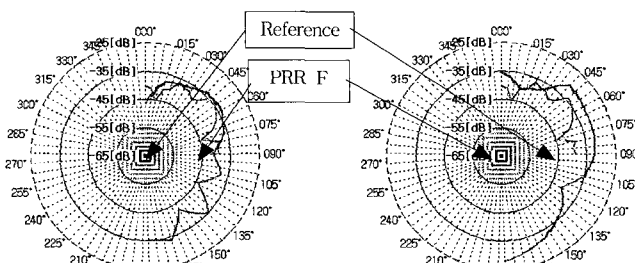
(c) Double Cylinder, Aluminum, $r=15$ cm, $l=45$ cm (d) Double Cylinder, Bronze, $r=15$ cm, $l=45$ cm

Fig. 7 Measurement results of PRR-S



(a)

(b)



(c)

(d)

Fig. 8 Measurement results of PRR-F

Fig. 8(a), (b), (c), and (d) are correspond to Fig. 5(a), (b), (c), and (d), respectively. All of the test samples in Fig. 8

show more high performance than that of the reference model. Further, the gain of test samples is to be considered large enough to have much real value in the practical use of fishing farm.

4. Conclusions

In the study, several radar targets are analysed based on the theoretical RCS approach, and two kinds of PRR models, PRR-F model for use in fisheries and PRR-S model for use in small sized ship, are designed and discussed their RCS performance.

Through the RCS measurement tests for the various sized samples, it was clearly shown that the conventional sphere-type shows optimum shape in case of PRR-S, while the cylinder-type which consists of large sized corner clusters or zig-zag flat plats gives best performance in case of PRR-F.

Acknowledgements

This work was partly supported by Fisheries Core Technology Program of the Ministry of Maritime Affairs and Fisheries in 2001.

References

- [1] Asoke K. Bhattacharyya, and D.L. Sengupta (1991), *Radar Cross Section Analysis & Control*, Artech House, pp.1-140
- [2] Bassem R. Mahafza (2000), *Radar Systems Analysis and Design Using MATLAB*. Champman & Hall/CRC, pp.71-140
- [3] Davis (2002), *Davis Echomaster & Emergency*, URL://www.davisnet.com
- [4] Eugene F. Knott (1993), *Radar Cross Section Measurement*, Van Nostrand Reinhold, New York, pp.1-26
- [5] IMO (1973), Resolution A.277(VIII), *Recommendation on Performance Standards for Radar Reflectors*, Adopted on 20 November 1973
- [6] IMO (1977), Resolution A.384(X), *Performance Standards for Radar Reflectors*, Adopted on 14 November 1977
- [7] IMO (2000), Sub-Committee on Safety of Navigation 46th Session, *Report to the Maritime Safety Committee, Annex 20: Draft Amendments to Chapter 13 of the HSC Code 2000*

- [8] J. B. Yim, H. R. Kim, K .D. Lee (2002a), "Research on the Required Specifications for the Ship's Sound Reproduction System According to SOLAS 2000," *Proc. of Summer Meeting 2002*, Acoustical Society of Korea, Vol.21(1s), pp.411-414
- [9] J. B. Yim, W. S. Kim (2002b) "Shaping Analysis to Decide the Design Condition of a Passive-type Radar Reflector," *J. of Korean Institute of Navigation and Port Research*, Vo.26(2), pp.199-208
- [10] Jim Coreman, Chuck Hawley, Dick Honey and Stan Honey (1995), *Radar Reflector Test*, URL://www.ussailing.org
- [11] Merrill L. Skolnik (2001), *Introduction to Radar Systems*, McGraw Hill, pp.30-98
- [12] National Institute of Standard Technology (2002), *Metrology for Radar Cross Section Systems*, URL://www.boulder.nist.gov
- [13] Ohio University (2002), *Current Reaseach: Compact Radar Measurement Range*, URL://esl.eng.ohio-state.edu
- [14] Ohio University (2002), *Antenna/RCS Measurement Workshop*, June, 2001, URL://esl.eng.ohio-state.edu
- [15] Rozendal Associates (2002), *Radar Reflectors*, URL//www.strandnet.com
- [16] SMI Fifth Annual Event (2001), *RCS Modeling and Analysis*, URL://www.naval-technology.com
- [17] W. S. Kim, Y. S. Ahn, I H. Kim, J. B. Yim. and S. H. Park (2002), "A Development of RADAR Reflector for Fishing Net Buoy," *Proc. of the 26th Annual Spring Meeting on Navigation and Port Research 2002*, Korean Institute of Navigation and Port Research, pp.177-184
-
- Received** 29 May 2003
Accepted 3 August 2003